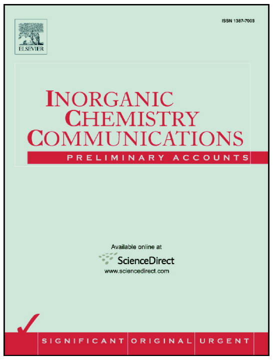

Syntheses, crystal structures, spectroscopy, and catalytic properties of two nickel-based hexaazamacrocyclic complexes with carboxylate ligands

Surachai Kongchoo, Kittipong Chainok, Anob Kantacha, Sumpun Wongnawa

PII: S1387-7003(17)30264-2
DOI: doi: 10.1016/j.inoche.2017.06.024
Reference: INOCHE 6691

To appear in: *Inorganic Chemistry Communications*

Received date: 2 April 2017
Revised date: 17 June 2017
Accepted date: 28 June 2017

Please cite this article as: Surachai Kongchoo, Kittipong Chainok, Anob Kantacha, Sumpun Wongnawa , Syntheses, crystal structures, spectroscopy, and catalytic properties of two nickel-based hexaazamacrocyclic complexes with carboxylate ligands, *Inorganic Chemistry Communications* (2017), doi: 10.1016/j.inoche.2017.06.024

Syntheses, Crystal Structures, Spectroscopy, and Catalytic Properties of Two Nickel-Based Hexaazamacrocyclic Complexes with Carboxylate Ligands

Surachai Kongchoo[a], Kittipong Chainok[b], Anob Kantacha[c], Sumpun Wongnawa[a,*]

[a] Department of Chemistry, Faculty of Science, Prince of Songkla University, Hat Yai, Songkhla, 90112, Thailand.

[b] Department of Physics, Faculty of Science and Technology, Thammasat University, Khlong Luang, Pathum Thani,12120, Thailand.

[c] Department of Chemistry, Faculty of Science, Thaksin University, Papayom, Phatthalung, 93110, Thailand.

* To whom correspondence should be addressed:

E-mail address: sumpun.w@psu.ac.th

GRAPHICAL ABSTRACT

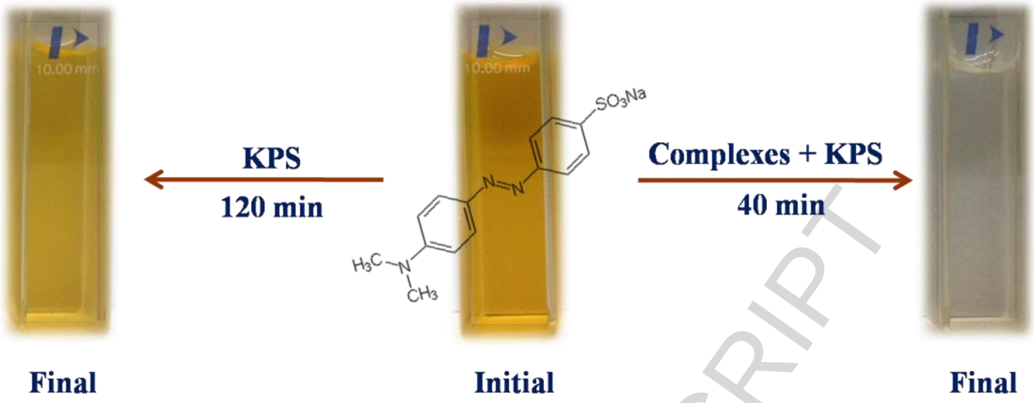

HIGHLIGHTS

- Straightforward synthesis with high yield
- Only small amount required in the degradation reaction
- Degradation reaction proceeded faster than without the catalyst
- Highly recyclable and robust

GRAPHICAL ABSTRACT - SYNOPSIS

$[NiL^1](ClO_4)_2$ and $[NiL^2](ClO_4)_2$ complexes were synthesized and used as precursor to synthesize $[NiL^1(4\text{-nba})_2]$ and $[NiL^2(sal)_2]$ complexes which were characterized with various techniques and X-ray diffraction analysis. Subsequently, the catalytic properties of both complexes in the degradation of methyl orange were investigated.

ABSTRACT:

Two new hexaazamacrocyclic nickel(II) complexes with the formula [NiL^1(4-nba)$_2$] **(1)** and [NiL^2(sal)$_2$] **(2)** (L^1 = 3,10-dioctyl-1,3,5,8,10,12-hexaazacyclotetradecane, L^2 = 3,10-diisobutyl-1,3,5,8,10,12-hexaazacyclotetradecane, 4-nba = *p*-nitrobenzoate, and sal = salicylate) were synthesized at room temperature. These complexes were characterized by physico-chemical and spectroscopic methods as well as single-crystal X-ray diffraction analysis. The coordination geometry in complexes **1** and **2** exhibit a distorted octahedron around the nickel(II) ion with hexaazamacrocyclic unit in the equatorial positions and two *p*-nitrobenzoate (or salicylate) anions in the axial positions. The degradation of methyl orange by potassium persulfate (KPS) in the presence of complex **1** (or **2**) oxidation system occurred to near completion in 60 min compared to only 55 % with KPS alone under UV light irradiation. Thus, both complexes in cooperation with KPS could be an attractive choice for degradation of organic pollutants for environmental remediation.

KEYWORDS: Nickel(II) complexes; Crystal structures; π-π stacking interactions; Persulfate activation; Methyl orange degradation; Advanced oxidation process

The increasing world population with growing industrial demands has led to a situation where protection of the environment has become a major problem and an importance factor for several industrial processes. Needless to say, the dye pollutants from textile industry are among those important sources of environmental contaminations. The resulting colored wastewater imposes a major problem for the industry as well as a serious threat to the environment [1,2]. Many studies have been carried out in which chemical and physical processes such as electrochemical process, ion-exchange, flocculation and coagulation technique, biological treatment, adsorption on activated carbon have been applied for color removal from textile wastewater [3-5].

Moreover, the advanced oxidation processes, or the so-called “AOPs”, have been widely studied for the treatment of industrial wastewaters. In general, AOPs are mainly based on the generation of the highly reactive oxidizing species, hydroxyl radical, which may be generated by various methods such as UV photolysis of hydrogen peroxide/ozone (H_2O_2/O_3) [6], photochemical catalysis (UV/TiO_2) [7], Fenton’s reaction [8], and persulfate oxidation [9,10]. The activated persulfate oxidation uses persulfate anion ($S_2O_8^{2-}$) which is also known as peroxydisulfate or peroxodisulfate. Persulfate salts of $(NH_4)_2S_2O_8$, $Na_2S_2O_8$, and $K_2S_2O_8$ dissociate in water to yield the persulfate anion which is one of the very strong oxidation species with high potential (E^o = 2.01 V) compared with H_2O_2 (E^o = 1.76 V). It shows some advantages over other oxidants as being a solid chemical at room temperature with the ease of storage and transport, high stability, high aqueous solubility, and relatively low cost [11]. There are several methods to activate the persulfate anions, such as thermal activation [12], UV irradiation [13], base activation [14], and activation with transition metal catalysts [15], to generate reactive sulfate radicals ($SO_4^{\cdot-}$). Activation of persulfate by metal ion catalysis occurs by an oxidation - reduction reaction in which low valent metal ions (M^{n+}) act as electron donors. Heterogeneous catalysis of the nickel(II) complexes with N-donor atoms from the hexaazamacrocyclic and carboxylate mixed ligands have been extensively used in the preparation of coordination polymers (CPs) [16,17]. In the family of aromatic carboxylate ligands, for example, 1,3,5-benzenetricarboxylate (BTC^{3-}), 2,2′-biquinoline-4,4′-dicarboxylate ($BQDC^{2-}$), and isonicotinnate the coordination network through space in one-, two- or three-dimensional architectures have been reported [18,19]. The dimensionality of the resulting coordination network can be increased by non-covalent interactions, such as hydrogen bonding, $\pi\cdots\pi$ stacking, C-H$\cdots\pi$, and other van der Waals interactions [20]. The coordination polymers have been an active research area in recent years because it can be applied in many fields such as magnetism, electronics, luminescence, and catalytic activity [21,22].

In this report, we describe the syntheses, characterizations, and crystal structures of two nickel(II) complexes, that is, $[NiL^1(4\text{-nba})_2]$ (**1**) and $[NiL^2(sal)_2]$ (**2**) (L^1 = 3,10-dioctyl-1,3,5,8,10,12-hexaazacyclotetradecane, L^2 = 3,10-diisobutyl-1,3,5,8,10,12-hexaazacyclotetradecane, 4-nba = *p*-nitrobenzoate, and sal = salicylate). In addition, catalytic capabilities of these complexes working in cooperation with persulfate (from KPS) for the degradation of methyl orange (MO) were investigated. For the preparation, **1** and **2** were synthesized at room temperature in mixed MeCN/H_2O solvent with triethylamine added for adjusting the pH of the solution (See supporting information). The carboxylate ligands replaced the perchlorate anions in the axial positions of both complexes. It is worth mentioning that during the reaction of complex **2**, the acetoxy group of the aspirinate ligand underwent hydrolysis process resulting in the cleavage of a covalent bond in a molecule to give the salicylate ligand which was confirmed in the structure by X-ray diffraction technique.

Single crystal X-ray diffraction analysis (See supporting information) showed that **1** crystallizes in the monoclinic space group of *C*2/c and containing $[NiL^1]^{2+}$ cation and two *p*-nitrobenzoate anions as shown in Fig. 1a and packing diagram in Fig. 1c. The nickel(II) ion of **1** is in a distorted octahedral geometry by binding to the four secondary nitrogen atoms of the hexaazamacrocycle (Ni(1)-N(1) = 2.0562(19) and Ni(1)-N(3) = 2.0720(2) Å) forming the equatorial plane in a square planar fashion and the distances are comparable to other hexaazamacrocycle Ni(II) complexes with Ni-N distances in the range 2.0535(2)-2.0729(13) Å [23,24]. Two oxygen atoms from two *p*-nitrobenzoate anions are located at the axial positions (Ni(1)-O(1) = 2.1407(15) and Ni(1)-O(1)^i = 2.1407(15) Å). The six-membered chelate ring (N(1)-Ni(1)-N(3) = 93.98(8)^o and N(1)^i-Ni(1)-N(3)^i = 93.98(8)^o) adopt *chair* conformation and the five-membered chelate ring assume *gauche* conformation (N(1)-Ni(1)-N(1)^i = 85.96(11)^o and N(3)-Ni(1)-N(3)^i = 86.09(11)^o) [30]. The C-N-C angles of the tertiary nitrogen atoms (N3 and its equivalent atoms) are in the range of 113.63(3)-118.13(4)^o which are larger than the ideal tetrahedral angle (109.5^o). Thus, the tertiary nitrogen atoms (N3) could use the sp^2-like hybridization similar to the other hexaazamacrocyclic complexes containing uncoordinated tertiary amino groups [25,26].

The structure of **1** shows intramolecular interactions of N-H···O hydrogen bonds between the secondary amine groups of the hexaazamacrocyclic ligand and the oxygen atoms of carbonyl group on the *p*-nitrobenzoate ion (N(1)-H(1)···O(2) = 2.070Å and ∠(N1)(H1)(O2) = 149^o) and the intermolecular interactions of N-H···O hydrogen bonds between the nitrogen atoms of secondary amine groups and the oxygen atoms of nitro group on the *p*-nitrobenzoate anions (N(3)-H(3)···O(4)^{ii} = 2.28Å and ∠(N3)(H3)(O4)^{ii} (-x+1/2, -y+1/2, -z+1) = 145^o). The average bond lengths and bond angles of **1** are very similar to those of previously reported [Ni($C_{16}H_{38}N_6$)(nicotinate)$_2$] complex [27]. In addition, there are face-to-face π-π stacking interactions at the distance 3.894 Å. These hydrogen bonds and π-π stacking interactions in **1** influence the stability of the structure which, finally, generating a one-dimensional network structure as shown in Fig. 1b.

(a)

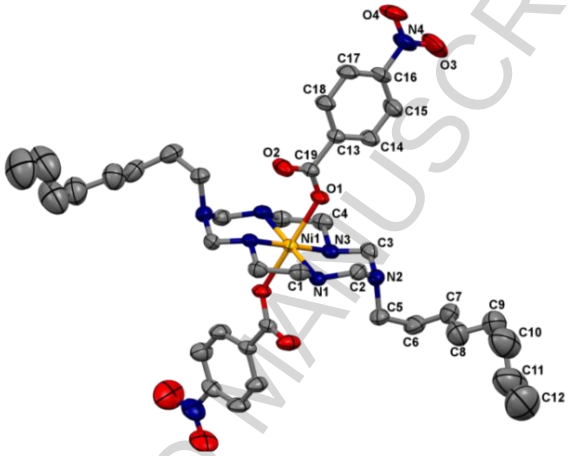

(b)

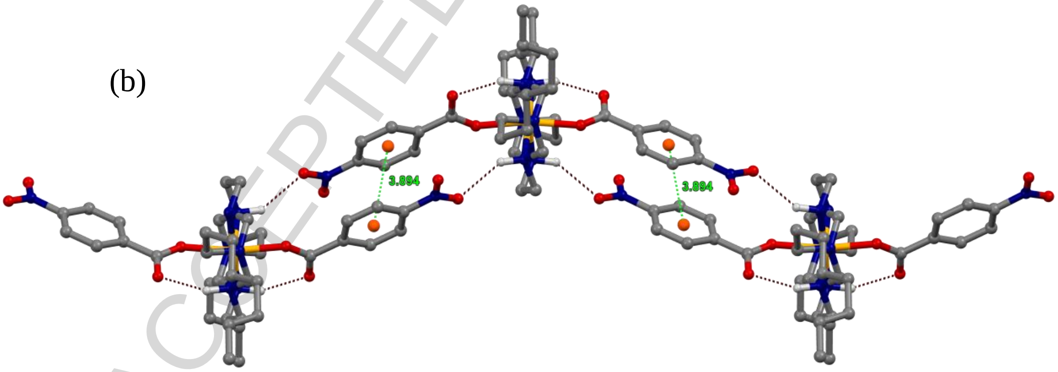

(c)

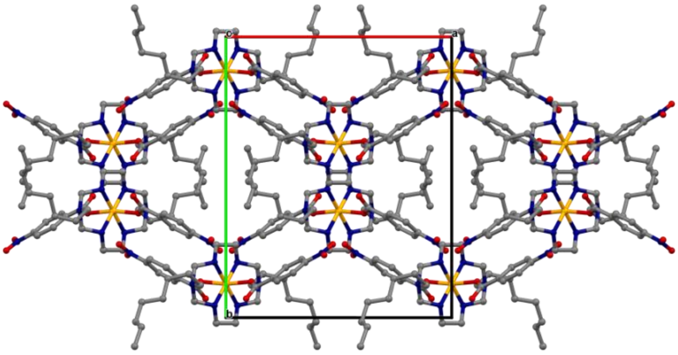

Fig. 1. Molecular structure of **1**, (a) Coordination environment of a mononuclear Ni(II) ion with the numbering scheme. (b) The 1D supramolecular network *via* the H-bonding and π-π stacking interactions. (c) The packing unit cell, viewed along the *a* axis.

From the X-ray single crystal diffraction analysis (See supporting information), complex **2** crystallizes in the monoclinic system with space group $P2_1$/n. The structure asymmetric unit of **2** consists of a basic $[NiL^2]^{2+}$ cationic part (L^2 = 3,10-diisobutyl-1,3,5,8,10,12-hexaazacyclotetradecane) and two salicylate anions as shown in Fig. 2a. The molecular packing arrangement of **2** plotted along the *a* axis is shown in Fig. 2b. In the structure of **2**, each nickel(II) ion has a distorted octahedral geometry with the two secondary and two tertiary amines of the hexaazamacrocycle and two salicylate anions. The Ni(1)-N(2) (tertiary amines) distance of 3.301 Å is significantly longer than the average Ni(1)-N(1) and Ni(1)-N(3) (secondary amines) distances of 2.055 Å indicating no participation in the coordination. The average Ni-N distance (2.096 Å) in NiN_4 plane is significantly longer than in the square-planar geometry of $[Ni(L^{R,R})](ClO_4)_2$ ($L^{R,R}$ = 1,8-di((*R*)-α-methylnaphthyl)-1,3,6,8,10,13-hexaazacyclotetradecane) complex (Ni-N = 1.941 Å) [28] but is similar to that observed for the octahedral nickel(II) complexes with 14-membered hexaazamacrocyclic ligands [29]. Moreover, C-N (tertiary amines) bond distances are much shorter than other C-N single bond distances indicating possibility of the sp^2-like hybridization of the uncoordinated tertiary nitrogen. The bond angles of the six-membered rings (N(1)-Ni(1)-N(3) = 94.10(7)^o and N(1)^i-Ni(1)-N(3)^i = 94.11(7)^o) are large than those of the five-membered rings (N(3)-Ni(1)-N(1)^i and N(3)^i-Ni(1)-N(1) = 85.89(7)^o). The axial Ni(1)-O(1) bonds are not quite perpendicular to the NiN_4 equatorial plane as the O(1)$_{axial}$-Ni(1)-N$_{equatorial}$ angles ranging between 88.80(7)-93.09(6)^o. Interestingly, the secondary amines of the hexaazamacrocyclic ligand form intramolecular hydrogen bonds with carboxylate oxygen atoms [N(3)-H(3A)···O(2)^i = 1.96 Å and 151^o; symmetry code: (i) -x+2, -y+1, -z+1] and hydrogen atoms of the hydroxyl groups of the salicylate ligand [O(3)-H(3)···O(2) = 1.77 Å and 147^o] and weak interactions of hydroxyl oxygen atoms of the salicylate ligand with the adjacent of the hydrogen atoms of the *i*-butylamine act as pendant arms [C(6)-H(6)···O(3)^{ii} = 2.51 Å and 165^o; symmetry code: (ii) -x+1, -y+1, -z+1], as shown in Fig. 2b.

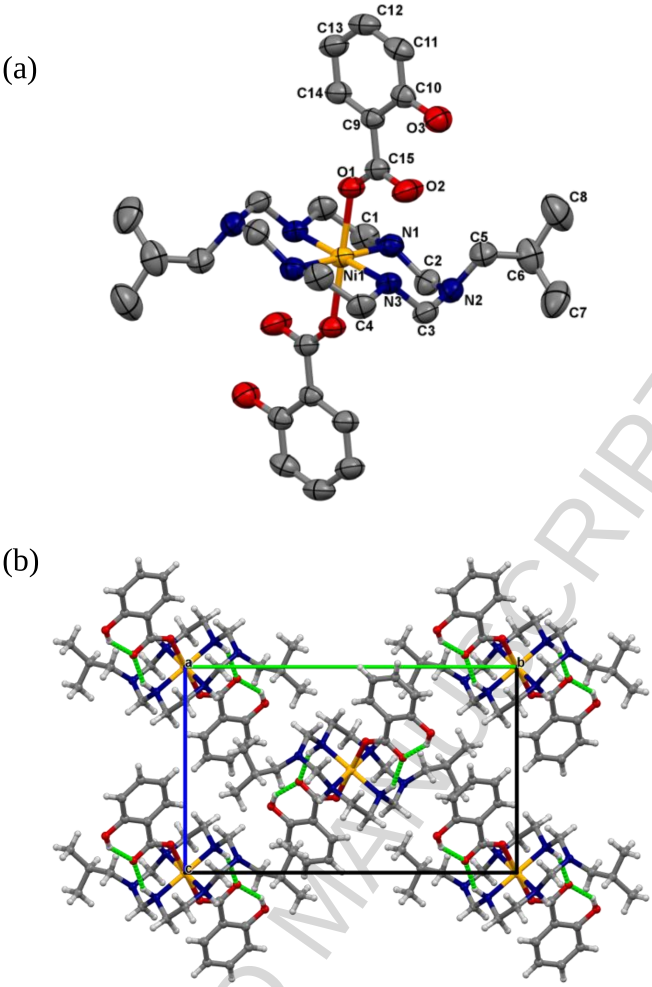

Fig. 2. Molecular structure of **2**, (a) Coordination environment of a mononuclear Ni(II) ion with the numbering scheme. (b) The packing unit cell, viewed along the *a* axis.

PXRD pattern was used to check the phase purity of **1** and **2** (Figs. S1 and S2). It can be seen that all the peaks present in the measured patterns match the simulated patterns from the single crystal diffraction data indicating the homogeneity of the bulk synthesized material and the as-grown crystals. The FT-IR spectrum (Fig. S3) of **1** shows very strong bands at 3301 and 3186 cm^{-1} that are assigned to the coordinated secondary amine groups. The bands around 2926-2853 cm^{-1} can be assigned to sp^2 C-H stretching mode of hexaazamacrocyclic ligands. The sharp vibrations at 1590 and 1340 cm^{-1} can be assigned to the C-O of a *p*-nitrobenzoate ion [27]. The weak band at 723 cm^{-1} is assigned to δ(C-H) of long chain alkyl group of the pendant arm [30]. The bands at 517 and 429 cm^{-1} can be assigned to the Ni-O and Ni-N, respectively [31]. The FT-IR spectrum (Fig. S4) of **2** shows very strong band at 3193 cm^{-1} due to the coordination of the secondary amine groups of hexaazamacrocyclic ligands. The C=O bands of the salicylate anions appear at 1597 and 1350 cm^{-1}, respectively.

The positions of these carboxyl group stretching vibrations and the separation between them are in the range expected for the monodentate carboxyl groups [32, 33]. In both complexes, no strong bands at 1068 and 621 cm^{-1} of the perchlorate anions from starting materials are present indicating the perchlorate has been replaced by carboxylate anions [30].

The thermal stability of **1** and **2** were examined by thermogravimetric analysis (TGA) in N_2 atmosphere from 50 °C to 1,000 °C, as shown in Fig. S5. Decomposition of **1** composed of the first weight loss 50.98 % in the range 230-323 °C corresponding to the loss of the macrocyclic ligand (calculated 51.92 %). On further heating, the second weight loss (40.61 %) was observed in the range 323-900 °C with the loss of *p*-nitrobenzoate ligand (calculated 39.82 %). Final residue, presumably a nickel oxide, 8.41 % was obtained (calculated: 8.26 %). The two steps decomposition was also observed for **2** from the TGA curve with the first weight loss of 47.93 % occurred within the range 249-355 °C corresponded to the release of the macrocyclic ligand (calculated 48.22%). The second weight loss of 41.87 % took place at 355-900 °C ascribable to the loss of salicylate ligand (calculated 42.66 %). The remaining weight corresponded to NiO was 10.20 % (calculated 9.12 %).

Persulfate oxidation, a member in the class of advance oxidation process, has been applied to degrade organic dyes such as crystal violet [11] and methyl orange [34]. Nevertheless, the uncatalyzed reaction efficiency is very low. In the presence of catalyst, persulfate oxidation proceeds via production of strongly oxidizing sulfate radicals. In this regard, the degradation efficiency of the catalytic oxidation of methyl orange was studied using KPS as an oxidant and complex **1** (or **2**) as heterogeneous catalyst. The degradation of methyl orange with KPS alone was slow with almost no change in color even up to 80 min of reaction (Fig. S6). However, when **1** (or **2**) was present the reaction took place almost immediately as indicated by the color change of methyl orange dye (Figs. S7 and S8). Under the same conditions, the photodegradation efficiency of **1** was higher than that of **2** (Fig. 3) which could be due to the directionality of metal-ligand interactions and the supramolecular interactions leading to formation of channels that could be accessed from the exterior allowing electron transfer and the incorporation of substrates inside the crystal. The reaction using **1** as catalyst could degrade 96 % of methyl orange in 60 min but only 83 % with **2**. With KPS alone, in the same time span, the degradation was only 55 %. This could be the result of the presence of **1** (or **2**) facilitated the generation of sulfate radicals from KPS to proceed more effectively. Recent reports of complexes of the same type, i.e. with large organic ligands, are those of Subramanian et al. 2015 [34] and Feng et al. 2014 [35]. The former reported the Ni(II) macrocyclic complex which could catalyse persulfate oxidative degradation of methyl orange. The Ni(II) complex could behave as homogeneous catalyst as well as heterogeneous catalyst by fixing it on adsorbents such as activated carbon or Amberlite. The degradation mechanism was proposed to proceed via the Ni(III) intermediate. The latter reported M(II) complexes (M = Zn, Cd) which behaved as heterogeneous catalysts working with persulfate in degradationof methyl orange. The key step was proposed as via M(III) intermediates. In the present work, complex **1** (and **2**) behaved as heterogeneous catalysts and we deemed that similar mechanism could be applied. The surface adsorbed $S_2O_8^{2-}$ anion accepted electron from solid complex **1** (or **2**) leading to the formation of transient Ni^{3+} in the solid complex which was quickly reduced back to Ni^{2+} complex after the completion of first cycle (Scheme 1) [15,36]. Meanwhile, the generated sulfate radicals went on to degrade the organic dyes. The sulfate radical is non-selective and strongly reactive oxidant. It has been shown that the sulfate radical could oxidize a wide variety of organic dyes pollutants such as Congo red [37-39] and methylene blue [40].

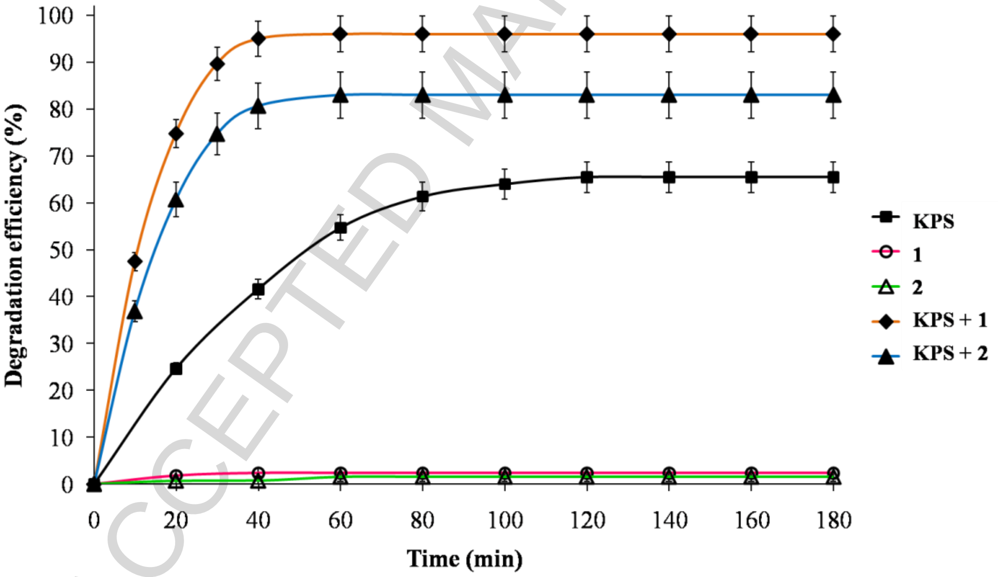

Fig. 3. Degradation efficiency (%) of methyl orange versus reaction time under UV irradiation.

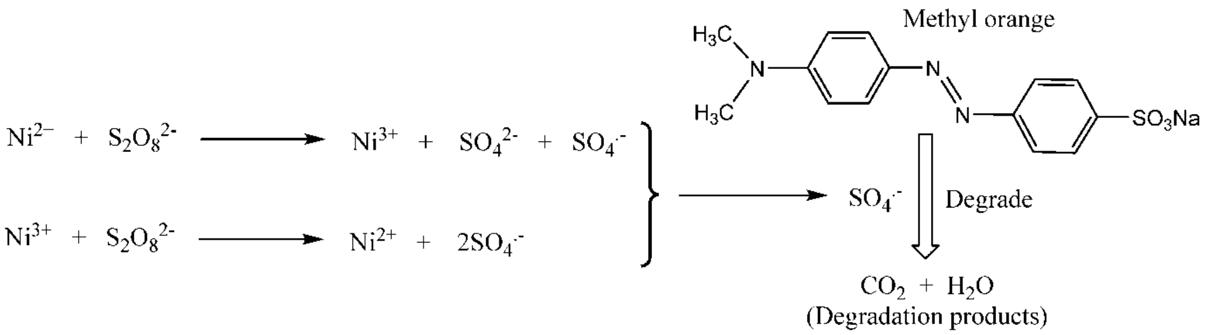

Scheme. 1. The proposed catalytic mechanism.

Both catalysts, **1** and **2,** are very robust as they survived unscratched through 5 cycles of recycling use. During the photodegradation tests, the catalyst could be simply isolated by centrifugation and reused by adding it into the freshly-prepared methyl orange solution to start the next round of photodegradation reaction. The efficiency of methyl orange degradation remained almost unchanged throughout 5 cycles of tests (Fig. 4) and not significantly lower than when it was first used (Fig. 3). The FT-IR spectra of the catalysts **1** and **2** isolated after the 5th cycle (Figs. S9 and S10) matched well with the initial spectra of both complexes (Figs. S3 and S4). The color of **1** remained unchanged both before and after the reaction while the color of **2** after used became almost undistinguishable paler than before used (Fig. S11)**.** All these results indicated that both **1** and **2** are attractive catalysts in terms of efficiency and robustness, especially complex **1** which showed higher efficiency than **2** while all the other data remained the same.

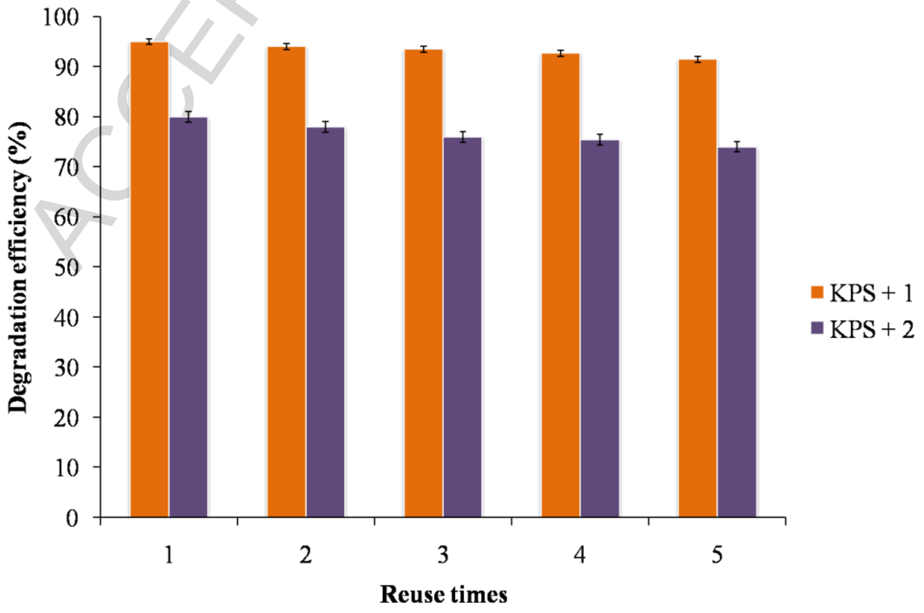

Fig. 4. The recyclability of complexes **1** and **2** with KPS as oxidant for the photodegradation of methyl orange solution under UV irradiation.

In conclusion, two new hexaazamacrocyclic nickel(II) complexes were synthesized and structurally characterized. The nickel(II) ions in **1** and **2** have a distorted octahedral geometry with hexaazamacrocyclic ligands in a planar conformation and *p*-nitrobenzoate (for **1**) and salicylate (for **2**) ions in the axial positions. The structure of **1** exhibiting a one-dimensional network is further interconnected by intramolecular N-H···O interactions between secondary amines and oxygen atoms of the *p*-nitrobenzoate ligand and intermolecular π-π stacking interactions. The salicylate ligand in the structure of **2** was the result from the cleavage of the aspirinate molecule during the synthesis reaction. These structures display intramolecular interaction between secondary amines and oxygen atoms of the salicylate ligand. In addition, the degradation of methyl orange with activation of persulfate in the presence of each complex showed that complex **1** had higher efficiency for the degradation of methyl orange dye than complex **2** within the same time span.

Acknowledgements

This work was supported by the Songklanagarind Scholarship for Graduate Studies from the Prince of Songkla University. We also thank the Department of Chemistry, Faculty of Science, Prince of Songkla University for supporting this research financially.

References

[1] N. Modirshahla, M.A. Behnajady, Dyes Pigm. 70 (2006) 54-59.

[2] L.M.D. Silva, W.F. Jardim, Quim. Nova 29 (2006) 310-317.

[3] B.R. Babu, A.K. Parande, S.A. Kumar, S.U. Bhanu, Open J. Safe. Sci. Technol. 1 (2011) 12-18.

[4] S.S. Moghaddam, M.R.A. Moghaddam, M. Arami, J. Hazard. Mater. 175 (2010) 651-657.

[5] K. Mahmoudi, N. Hamdi, A. Kriaa, E. Srasra, Russ. J. Phys. Chem. A 86 (2012) 1294-1300.

[6] J.-C. Geng, L. Qin, C.-H. He, G.-H. Cui, Transition Met. Chem. 37 (2012) 579-585.

[7] I.K. Konstantinou, T.A. Albanis, Appl. Catal. B 49 (2004) 1-14.

[8] S.H. Bossmann, E. Oliveros, S. Göb, S. Siegwart, E.P Dahlen, L. Payawan, M. Straub, M. Wörner, A.M. Braun, J. Phys. Chem. A 102 (1998) 5542-5550.

[9] X.-R. Xu, S. Li, Q. Hao, J.-L. Liu, Y.-Y. Yu, H.-B. Li, Int. J. Environ. Bioener. 1 (2012) 60-81.

[10] C. Qi, X. Liu, X. Zhang, J. Ma, H. Tan, W. Ye, Chem. Eur. J. 249 (2014) 6-14.

[11] S. Gokulakrishnan, P. Parakh, H. Prakash, J. Hazard. Mater. 213-214 (2012) 19-27.

[12] M. Nie, Y. Yang, Z. Zhang, C. Yan, X. Wang, H. Li, W. Dong, Chem. Eng. J. 246 (2014) 373-382.

[13] Y.-Q. Gao, N.-Y. Gao, Y. Deng, Y.-Q. Yang, Y. Ma, Chem. Eng. J. 195-196 (2012) 248-253.

[14] O.S. Furman, A.L. Teel, R.J. Watts, Environ. Sci. Technol. 44 (2010) 6423-6428.

[15] C.-H. Jiao, C.-H. He, J.-C. Geng, G.-H. Cui, Transition Met. Chem. 37 (2012) 17-23.

[16] J.-W. Cui, S.-X. Hou, K.V. Hecke, G.-H. Cui, Dalton Trans. 46 (2017) 2892-2903.

[17] S.Y. Hao, S.-X. Hou, K.V. Hecke, G.-H. Cui, Dalton Trans. 46 (2017) 1951-1964.

[18] T.-B. Lu, H. Xiang, R.L. Luck, Z.-W. Mao, D. Wang, C. Chen, L.N. Ji, Cryst. Eng. Comm. 41 (2001) 1-2.

[19] K.S. Min, M.P. Suh, Eur. J. Inorg. Chem. 2001 (2001) 449-455.

[20] J.-C. Geng, L. Qin, X. Du, S.-L. Xiao, G.-H. Cui, Z. Anorg. Allg. Chem. 638 (2012) 1233-1238.

[21] J.M. Hu, V.A. Baltov, B. Yu, K.V. Hecke, G.-H. Cui, Dalton Trans. 45 (2016) 2426-2429.

[22] G.P. Yang, L. Hou, X.-J. Luan, B. Wu, Y.-Y. Wang, Chem. Soc. Rev. 41 (2012) 6992-7000.

[23] J.H. Park, A.R. Jeong, D.K.A.K. Hastuti, M.J. Jeong, K.S. Min, J. Incl. Phenom. Macrocycl. Chem. 82 (2015) 153-162.

[24] J.H. Park, A.R. Jeong, J.W. Shin, M.J. Jeong, C.S. Cho, K.S. Min, Inorg. Chem. Commun. 57 (2015) 44-46.

[25] Y.-W. Li, H. Xiang, T.-B. Lu, S.W. Ng, Acta Crystallogr., Sect. E 60 (2004) 309-311.

[26] S. Han, T. Kim, A.J. Lough, J.C. Kim, Inorg. Chim. Acta 370 (2011) 170-174.

[27] J.W. Shin, D.-W. Kim, D. Moon, Polyhedron 105 (2016) 62-70.

[28] K.S. Min, M.J. Park, J.J. Ryoo, Chirality 25 (2013) 54-58.

[29] S.-G. Kang, K. Ryu, S.-K. Jung, J. Kim, Inorg. Chim. Acta 293 (1999) 140-146.

[30] S. Kongchoo, A. Kantacha, S. Saithong, S. Wongnawa, J. Chem. Crystallogr. 46 (2016) 222-229.

[31] J.C. Kim, J.A. Kim, Y.C. Kang, Transition Met. Chem. 31 (2006) 829-833.

[32] A.L. Abuhijleh, C. Woods, Inorg. Chem. Commun. 4 (2001) 119-123.

[33] G.B. Deacon, R.J. Phillips, Coord. Chem. Rev. 33 (1980) 227-250.

[34] G. Subramanian, P. Nalawade, S.J. Hinder, S.C. Pillai, H. Prakash, RSC Adv. 5 (2015) 31716-31724.

[35] Z.-Q. Feng, X.-L. Yang, Y.-F. Ye, J. Inorg. Organomet. Polym. 24 (2014) 684-693.

[36] L. Qin, S.L. Xiao, P.J. Ma, G.-H. Cui, Transition Met. Chem. 38 (2013) 627-633.

[37] J.-C. Geng, L.W. Liu, S.L. Xiao, G.-H. Cui, Transition Met. Chem. 38 (2013) 143-148.

[38] L. Qin, L.-W. Liu, X. Du, X., G.-H. Cui, Transition Met. Chem. 38 (2013) 85-91.

[39] Z.-T. Zhang, Y.Y. Wang, R. Yang, R. Liu, Y. Zhao, G.-H. Cui, Transition Met. Chem. 41 (2016) 169-178.

[40] C.-C. Wang, H.-P. Jing, P. Wang, J. Mol. Struct. 1074 (2014) 92-99.